J. Membrane Biol. 159, 219–229 (1997)

The Journal of
Membrane
Biology

Characterization of a Chloride-Selective Channel from Rough Endoplasmic Reticulum Membranes of Rat Hepatocytes: Evidence for a Block by Phosphate

A. Eliassi, L. Garneau, G. Roy, R. Sauvé
Department of Physiology, Membrane Transport Research Group, University of Montréal, C.P. 6128, Succ. Centre-ville, Montréal Canada H3C 3J7

Received: 10 January 1997/Revised: 29 May 1997

Abstract. We have characterized the conduction and blocking properties of a chloride channel from rough endoplasmic reticulum membranes of rat hepatocytes after incorporation into a planar lipid bilayer. Our experiments revealed the existence of a channel with a mean conductance of 164 ± 5 pS in symmetrical 200 mM KCl solutions. We determined that the channel was ten times more permeable for Cl^- than for K^+, calculated from the reversal potential using the Goldman-Hodgkin-Katz equation. The channel was voltage dependent, with an open probability value ranging from 0.9 at −20 mV to 0.4 at +60 mV. In addition to its fully open state, the channel could also enter a flickering state, which appeared to involve rapid transitions to zero current level. Our results showed a decrease of the channel mean open time combined with an increase of the channel mean closed time at positive potentials. An analysis of the dwell time distributions for the open and closed intervals led to the conclusion that the observed fluctuation pattern was compatible with a kinetic scheme containing a single open state and a minimum of three closed states. The permeability sequence for test halides determined from reversal potentials was $Br^- > Cl^- > I^- \approx F^-$. The voltage dependence of the open probability was modified by the presence of halides in *trans* with a sequence reflecting the permeability sequence, suggesting that permeant anions such as Br^- and Cl^- have access to an internal site capable of controlling channel gating. Adding NPPB to the *cis* chamber inhibited the channel activity by increasing fast flickering and generating long silent periods, whereas channel activity was not affected by 50 μM DNDS in *trans.* The channel was reversibly inhibited by adding phosphate to the *trans* chamber. The inhibitory effect of phosphate was voltage-dependent and could be reversed by addition of Cl^-. Our results suggest that channel block involves the interaction of HPO_4^{2-} with a site located at 70% of the membrane span.

Key words: Endoplasmic reticulum — Cl^- channel — Phosphate — Bilayer — Vesicles — Cl^- Channel in ER

Introduction

Chloride is the most abundant physiological anion. One of the key mechanisms responsible for the transport of Cl^- ions across biological membranes consists of pore-forming proteins through which Cl^- ions diffuse down their electrochemical gradient. Numerous studies have shown that the Cl^- channels localized at the plasma membrane of excitable and nonexcitable cells are involved in a large variety of cellular events including cell volume regulation [12], salt secretion processes [1, 6, 16] and modulation of membrane potential [7]. Cl^--selective channels have also been identified in intracellular organelles such as Golgi apparatus [9], lysosomes [30], endosomes [23], sarcoplasmic reticulum (SR) [21, 29] and mitochondria [5]. For instance, Cl^- selective channels of 55 pS (260 mM Cl^-) and 130 pS have been reported in two different bilayer studies on cardiac SR [21, 31] whereas a Cl^- channel of 505 pS in 200 mM Cl^- was identified by Palade and coworkers (1989) in membrane preparations of SR skeletal muscles [10]. Cl^- permeant channels have also been characterized in patch clamp experiments carried out on giant rough endoplasmic reticulum (RER) liposomes. This approach provided evidence for a voltage-sensitive Cl^- channel with a mean conductance of 260 pS (140 mM KCl on both sides), and for a voltage-insensitive channel also permeable to Cl^- ions but of smaller conductance (70 pS) [24]. The technique of vesicle fusion with a lipid bilayer was also used to identify a voltage-regulated double-barreled Cl^- channel of 160 pS in RER membranes from rat hepatocytes

Correspondence to: R. Sauvé

[15]. A kinetic analysis of this channel showed that this double-barreled system could be interpreted in terms of a model in which all the states resulting from the superposition of two independent monomeric channels have access to a common inactivated state. The physiological role of these channels remains to be confirmed in many cases, but several studies have already indicated that Cl^- channels in organelles may be involved in the release and/or uptake of Ca^{2+} and H^+ ions in intracellular stores by generating an opposite charge movement essential to maintaining electroneutrality [2, 18, 25].

Despite the intrinsic role of Cl^- selective channels to Ca^{2+} liberation and/or H^+ uptake-related processes in the ER, there is currently limited information on the biophysical properties and gating mechanisms of the Cl^- channels in ER structures. In this study, we used the channel incorporation technique to explore the ionic selectivity, activation processes and pharmacological profile of a Cl^- channel present in RER membranes from rat hepatocytes. Our results indicate that RER membranes contain a voltage-dependent Cl^- channel of 164 pS, the activity of which can be in part controlled by the permeant anions in *trans.*

Materials and Methods

Preparation of Membrane Vesicles

Rough microsomes (RM) derived from RER of rat liver cells were prepared as previously described [11, 15], with the exception that protease inhibitors (1 mM EDTA; 0.1 mM PMSF; 2 μM leupeptin and 10 μM pepstatin A) were added throughout the vesicle preparation procedure. RM were stored in 10 μl aliquots in 250 mM sucrose/3 mM imidazole, pH 7.4 at −80°C until used. The final concentration of RM ranged from 8 to 9 mg protein/ml and morphological measurements carried out by Paiement and Bergeron (1983), [17] confirmed that these vesicles were oriented in the right-side out configuration.

Bilayer Formation

Single-channel measurements were carried out using the chamber partition technique. Planar phospholipid bilayers were formed in a 300 μm-diameter hole drilled in a Delrin partition, which separated two chambers. The *cis* and *trans* chambers held respectively 5 ml and 3 ml of solution. The pH on both sides was adjusted to 7.4 with Tris-HEPES and the *cis* solution was always hyperosmotic relative to the *trans* solution as to improve vesicle fusion. The outline of the aperture was coated with triolein before the application of the lipid suspension to improve membrane stability. Planar phospholipid bilayers were painted using a 1:1 mixed suspension of POPC:POPE in decane at a final concentration of 20 mg lipid/ml. Fusion of the vesicles was initiated mechanically by gently touching the bilayer from the *cis* side using a small stainless steel wire (Kerr) of 150 μm diameter, on the tip of which was deposited a small drop of the vesicle-containing solution. Formation and thinning of the bilayer were monitored electrically. Typical capacitance values ranged from 400 pF to 500 pF. When required, perfusion of the *trans* chamber was carried out using a peristaltic perfusion pump set at 25 ml/min (Masterflex, Cole-Parmer Ins.).

Single-channel currents were measured with a BC-525A amplifier (Warner Instrument). The *trans* chamber was voltage-clamped relative to the *cis* chamber, which was grounded. Electrical connections were made by using Ag/AgCl electrodes and agar salt bridges (3M KCl) to minimize liquid junction potentials. Signals were stored on videotapes (SONY, SL-300) and subsequently transferred to a PC for off-line analysis. Recordings were digitized at sampling rates between 500 Hz and 3 kHz which corresponded to five times the cutoff frequencies chosen for filtering (8-pole Bessel: Frequency Devices 902). The unitary current amplitude and channel open probability were estimated from current amplitude histograms or from noise-free Markov signals generated by processing experimental current records using an algorithm based on the Baum-Welch reestimation formulae [15]. For multi-channel recordings, the open probability was calculated assuming that the current levels were distributed according to a binomial statistic. The validity of the binomial distribution was tested by performing a χ^2 analysis based on the procedure described previously [15]. All experiments were performed at room temperature (20° ± 2°C).

Chemical Reagents

All chemicals were obtained from commercial sources. POPC and POPE were obtained from Avanti Polar Lipids (Alabaster, AL) and decane from Fisher Scientific (Pittsburgh). Triolein, HEPES, NaH_2PO_4 and Tris were purchased from Sigma. NPPB and DNDS were obtained from RBI (Research Biochemicals International, Natick, MA). Salts and solvent were analytical grade. Salt solutions were filtered through microfilters with a pore size of 0.2 μm (Millipore Corporation, Boston, MA).

Abbreviations

DNDS:	4,4′-dinitrostilbene-2,2′-disulfonic acid
HEPES:	N-2-Hydroxylethylenepiperazine-N′-2-ethanesulfonic acid
NPPB:	5-nitro-2-(3-phenylpropylamine)benzoic acid
PG:	Phosphatidylglycerol
PMSF:	Phenylmethylsulfonyl Fluoride
POPC:	1-palmitoyl-2-oleoylphosphatidylcholine
POPE:	1-palmitoyl-2-oleoylphosphatidylethanolamine
Tris:	Tris(hydroxymethyl)aminomethane

Results

Cl^- Single-Channel Characteristics

Figure 1*A* shows examples of current fluctuations obtained following the incorporation of liver RER vesicles into a planar lipid bilayer. Channel incorporation was carried out in asymmetric Cl^- conditions (200 mM KCl *cis*/50 mm KCl *trans*), and the resulting single channel activity recorded at the various membrane voltages indicated. Experiments performed under these conditions showed a significant increase of the current jump amplitude for applied potentials positive to −30 mV, but clear single-channel events could not be unambiguously recorded at more negative potential values. Despite these limitations, the results in Fig. 1*A* indicate a zero current potential value close to −34 mV, the equilibrium potential expected for Cl^- ions under the prevailing ionic con-

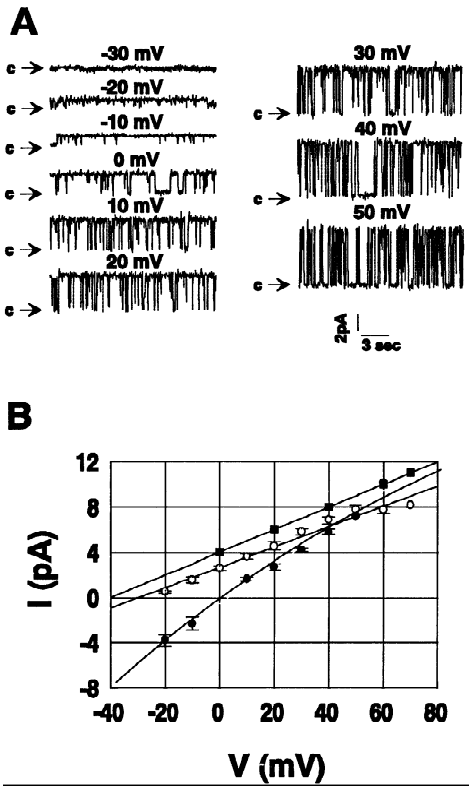

Fig. 1. (*A*) Examples of single-channel currents recorded following fusion of RER vesicles from rat hepatocytes into a planar bilayer. Single-channel currents recorded in 200 mM KCl *cis*/50 mM KCl *trans* conditions at potentials ranging from −30 to +50 mV. Current traces filtered at 400 Hz and sampled at 2 kHz. The letter *c* indicates the closed-state current level. (*B*) Single-channel current-voltage relationship measured in various *trans* Cl^- concentrations: 200 mM KCl *cis*/50 mM KCl *trans* (○); 200 mM KCl *cis*/200 mM KCl *trans* (●); and 200 mM KCl *cis*/10 mM KCl *trans* (■). The mean slope conductances for positive currents corresponded to 90 ± 12 pS (○), 164 ± 5 pS (●) and 100 ± 2 (■) respectively. The zero current potentials indicate a permeability ratio $P_{Cl}/P_K > 10$. Data points are mean ± SD from 4 (○), and 2 (●,■) experiments.

ditions. In addition, channel fluctuations appeared as long channel openings interrupted by fast flickering transitions to the zero current level. The channel-gating behavior was voltage dependent with increased channel flickering separated by longer silent periods at increasingly positive potential values. Spontaneous subconductance states with current amplitudes corresponding to 1/2 to 3/4 of the full conductance level were occasionally recorded (*data not shown*). Because these subconductance levels were rarely observed their contribution to the overall channel fluctuation pattern was not considered.

To investigate the channel current-voltage (*I/V*) relationship and Cl^--selectivity, experiments were undertaken in which the *cis* Cl^- concentration was kept at 200 mM while varying the Cl^- concentration in the *trans* chamber. Figure 1*B* shows the resulting channel *I/V* curves for different Cl^- concentrations. Under symmetrical 200 mM KCl conditions (filled circles), the channel *I/V* curve appeared slightly rectifying with a mean slope conductance for inward currents of 164 ± 5 pS ($n = 2$). Furthermore Fig. 1*B* shows that a decrease of the *trans* Cl^- concentration caused a shift of the reversal potential towards more negative values (trans relative to *cis*). For instance, in 200 mM Cl^- *cis*/50 mM Cl^- *trans* conditions (open circles), the mean reversal potential from four different bilayers was estimated at −28 ± 3 mV. This value is in agreement with the Nernst equilibrium potential expected for a Cl^- selective channel ($E_{Cl^-} = -34$ mV) and corresponds to a permeability ratio $P_{Cl}/P_K > 10$ as calculated on the basis of the Goldman-Hodgkin-Katz equation. This conclusion was further substantiated in experiments carried out in 200 mM *cis*/10 mM *trans* KCl (filled squares) for which extrapolated zero current potential values more negative than −45 mV were obtained ($n = 2$). Precise estimations of the zero current potential could not, however, be obtained under these experimental conditions due to the absence of reliable inward current measurements with 10 mM KCl in the *trans* chamber.

Channel Kinetic Properties

The channel kinetic properties were investigated by measuring on stationary single channel records dwell time distributions for the open and closed states. Examples of the resulting distributions where time intervals were bined according to a logarithmic scale are illustrated in Fig. 2. Time intervals were measured either by generating noise-free current records according to the Baum-Welch reestimation formulae, or by using the double threshold procedure described in Bellemare et al., (1992) [3] on original current traces. The stationarity of the recorded signal was tested according to the criteria defined in Denicourt et al., (1996) [6]. This analysis provided clear evidence for a kinetic pattern characterized by a single open state for time intervals ranging from 1 msec to 1 sec. This conclusion was also supported by an analysis of multi-channel current records such as the one shown in Fig. 3*A*, where the distribution of time intervals resulting from the simultaneous opening of all the channels present could be fitted to a single exponential function. In contrast, the closed time distributions measured from recordings containing a single channel, required a minimum of three exponential functions to be properly fitted, indicating a minimum of three closed states. Attempts to curvefit these distributions with two exponential functions only were clearly unsatisfactory. Furthermore, there was a marked effect of the voltage on the dwell time interval distributions for the closed states with an increase of the time constants and a greater contribu-

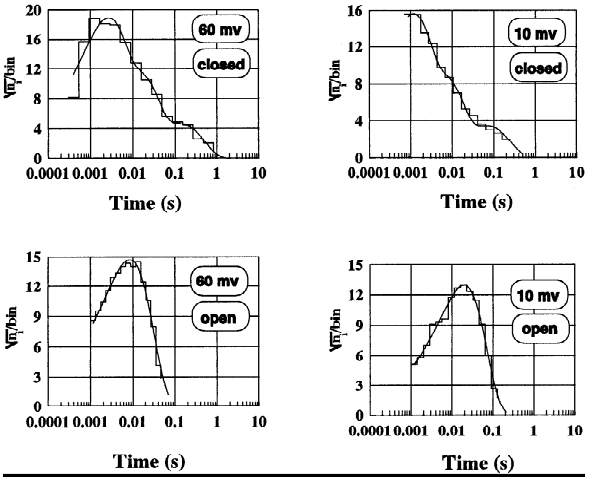

Fig. 2. Dwell time distributions for the open and closed states at +60 and +10 mV. The open time distribution was fitted to a single exponential function while three exponentials were required to account for the closed time interval distributions. The dwell time distribution appeared voltage-dependent with the channel mean open time decreasing from 25 msec at 10 mV to 8 msec at 60 mV, and the characteristic times for the closed interval distributions varying from 1.5 msec, 10 msec and 150 msec at 10 mV to 2.5 msec, 20 msec and 400 msec at 60 mV respectively.

tion of the long closures at positive potentials. The time interval distribution for the open state also appeared affected by the voltage, such that the characteristic time of the dwell time distribution was reduced at positive potential values.

Voltage Dependence of Open Probability

The effect of voltage on the channel-gating properties was next investigated by measuring the channel open probability (P_o) either directly from current recordings containing a single channel (Fig. 1*A*) or through a binomial analysis of current records with multi-channels (Fig. 3*A*). In experiments where a single channel was detected, the voltage dependence of P_o during bursting activity was also estimated by computing P_o values after omission of silent periods >100 msec. This threshold value was selected since it guarantees that more than 90% of the long closed time intervals were omitted, without appreciable effects (0.6%) on the intermediate (20 msec) and short closed interval (2 msec) distributions (Fig. 2). Figure 3*B* illustrates the relationship between P_o and membrane potential measured from four different experiments in asymmetrical solutions (200 mM KCl *cis*/50 mM KCl *trans*). The results show global P_o estimations reaching values close to 0.9 within the potential range ± 20 mV and a decrease of the channel P_o at more positive potential values. A similar voltage dependence was observed using current records in which long closures were systematically omitted, an indication that the observed voltage dependence is not exclusively related to the appearance of long silent periods. These data were fitted to a Boltzmann distribution according to:

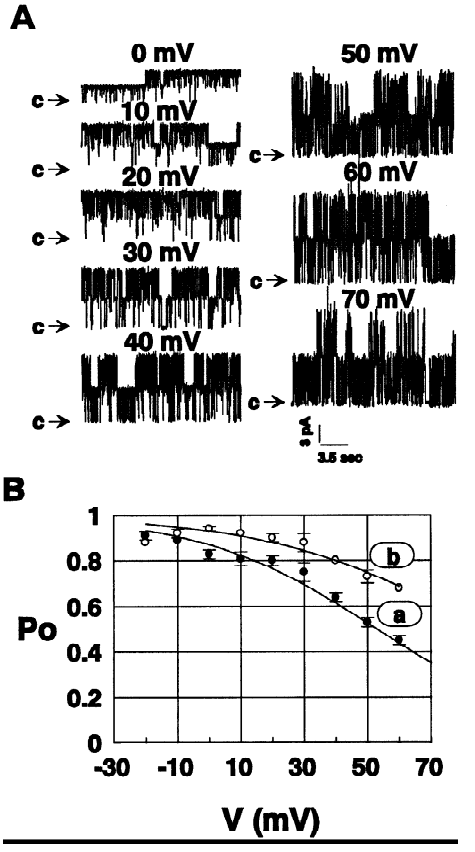

Fig. 3. (*A*) Effect of membrane voltage on channel-gating behavior measured from current records containing multiple channels. Single-channel recordings obtained in the presence of 200 mM KCl *cis*/50 mM KCl *trans.* Long interburst silent periods and faster flickering are observed at high positive potentials. (*B*) Channel open probability (P_o) at different membrane voltages. Open channel probability as a function of voltage computed from current records with (●, $n = 4$), (*a*), or without (○, $n = 3$) (*b*) inclusion of long silent periods (>100 msec). Measurements were carried out under asymmetrical 200 mM KCl *cis*/50 mM KCl *trans* conditions. Theoretical curves were calculated according to equation (1) with $V_o = 52$ mV and $Zq = 0.90$ for *a* and $V_o = 86$ mV and $Zq = 0.77$ for *b.*

$$P_o = \frac{1}{1 + e^{\frac{Zq(V - V_o)}{KT}}} \qquad (1)$$

where Zq is the apparent gating charge, V is the membrane voltage, V_o the voltage for half activation, K and T, the Boltzmann's constant and the temperature, respectively. This procedure led to V_o equal to 52 and 86 mV for curves *a* and *b*, respectively, with Zq values within the range 0.83 q − 0.97 q in *a* and 0.67 q − 0.87 q in

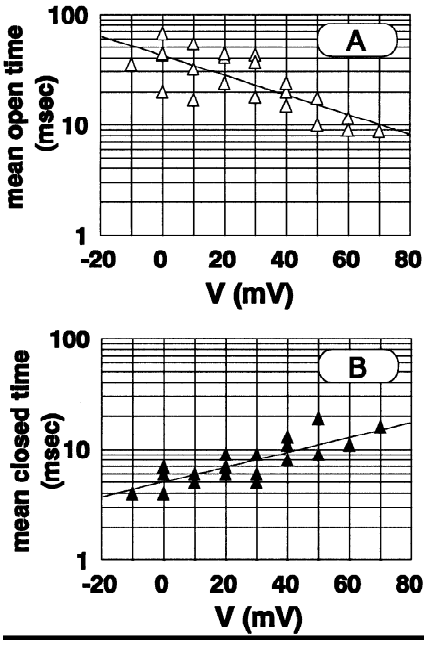

Fig. 4. Variation of the channel mean open time and mean closed time as a function of voltage from 3 experiments. Mean open time decreased within the voltage range −10 to +70 mV, whereas mean closed time increased over the same voltage span.

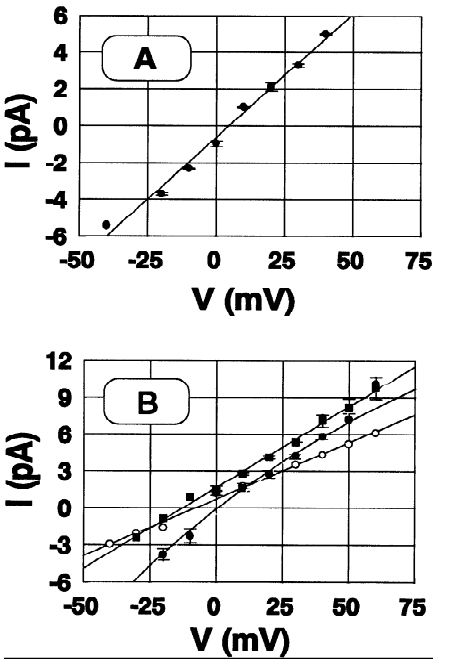

Fig. 5. *I-V* relationship with different halides in the *trans* chamber. (*A*) Single-channel *I/V* curves were measured in the presence of 200 mM KCl *cis*/50 mM KCl + 150 mM KBr *trans*. *(B)* Single-channel *I/V* relationships measured in the presence of 200 mM KCl *cis*/200 mM KCl *trans* (●); 200 mM KCl *cis*/50 mM KCl + 150 mM KI *trans* (○); and 200 mM KCl *cis*/50 mM KCl + 150 mM KF *trans* (■).

b. Figure 4 shows the variation of the channel mean closed time and mean open time as a function of voltage computed from three different experiments. These results confirm a reduction of the channel mean open time coupled to an increase of the channel mean closed time at positive potentials. The observed voltage dependence of the mean closed time supports the results already presented in Fig. 2, where each of the time constants for the closed interval distribution was found to increase at positive potential values. These observations provide evidence that the voltage dependence of P_o does not depend exclusively on the appearance of long channel closures at positive potentials (Fig. 2) but also involves a decrease of the channel open time and an increase of the channel mean closed time during channel bursts.

Anion Selectivity

The channel selectivity for different halides was examined by measuring current-voltage relations and zero current reversal potentials in experiments where the *cis* solutions were kept at 200 mM KCl, while *trans* solutions contained 50 mM KCl plus 150 mM of the test halide potassium salt. Under these conditions, a permeability ratio P_x/P_{Cl} of 1, where P_x represented the ionic permeability of the test halide, would lead to a reversal potential equal to zero mV. The results are presented in Fig. 5*A* and *B* respectively. In control conditions, corresponding to symmetrical 200 mM Cl^- concentrations, the *I/V* curve intersected the voltage axis at zero mV as expected (Fig. 5*B*, filled circles). However, none of the *I/V* curves measured with the different halides studied resulted in an identical reversal potential value, indicating that the permeability of the test halides differ from that obtained for Cl^- ions. For instance, Fig. 5*A* shows that the reversal potential was shifted to +5 ± 0.7 mV ($n = 2$) when Cl^- was substituted by Br^-, a result compatible with bromide being more permeant than Cl^-. In contrast, the *I/V* curves (Fig. 5*B*) obtained with 150 mM I^- (open circles) or F^- (filled squares) in *trans* intersected the voltage axis at −14 ± 6 mV ($n = 2$) and −12 ± 5 ($n = 2$), respectively, for an overall permeability sequence $P_{Br} > P_{Cl} > P_I \approx P_F$. The Table presents the zero current reversal potentials and unitary channel conductances for the halide ions indicated in Fig. 5*A* and *B* and the associated permeability ratios relative to Cl^-, computed according to the Goldman-Hodgkin-Katz equation. The single-channel conductance measured at positive potentials in the presence of 150 mM I^- in *trans* appeared markedly smaller than the conductance values obtained with Br^-, Cl^- and F^-. For instance, the conductance for I^- and F^- were estimated at 80 ± 14 pS and 140 ± 14 pS respectively, despite having nearly equivalent permeability ratios. This latter observation suggests that, in con-

Table 1. Shift in reversal potentials, permeability ratios, and conductances for various halogen anions

	Chloride	Fluoride	Bromide	Iodide
Shift of reversal potential (mV)	0 ± 4 $n = 2$	-12 ± 5 $n = 2$	5 ± 0.7 $n = 2$	-14 ± 6 $n = 2$
Conductance (pS)	164 ± 5 $n = 2$	140 ± 14 $n = 2$	146 ± 2 $n = 2$	80 ± 14 $n = 2$
P_X/P_{Cl}	1	0.5	1.3	0.45

Reversal potentials were measured with the *cis* and *trans* solutions containing respectively, 200 mM KCl and 50 mM KCl plus 150 mM of the test halide K salt (KX). The resulting permeability sequence corresponded to $Br^- > Cl^- > I^- \approx F^-$.

trast to the other halides, I^- ions can interact with the channel so as to reduce the single-channel conductance.

To determine whether channel gating was affected by permeant halides, experiments were performed where the *cis* solution remained at 200 mM KCl, while *trans* solutions contained 50 mM KCl plus 150 mM of the test halide. Figure 6*A* and *B* present the voltage dependence of the channel open probability as a function of voltage for each halide. The effect of voltage on P_o appeared markedly stronger when F^- (filled squares) was present in *trans* as compared to Br^- (open triangles) and I^- (open circles). The mean value of P_o was found to increase with *trans* Br^- and I^-, indicating that these anions modify the channel gating process in addition to their effect on the channel current amplitude. In contrast, the voltage dependence of P_o measured using 150 mM F^- + 50 mM Cl^- in *trans* did not differ significantly from that obtained in control 200 mM Cl^- *cis*/50 mM Cl^- *trans* conditions. These results suggest that permeant anions present in *trans* may have access to a site which, when occupied, leads to a greater open channel probability.

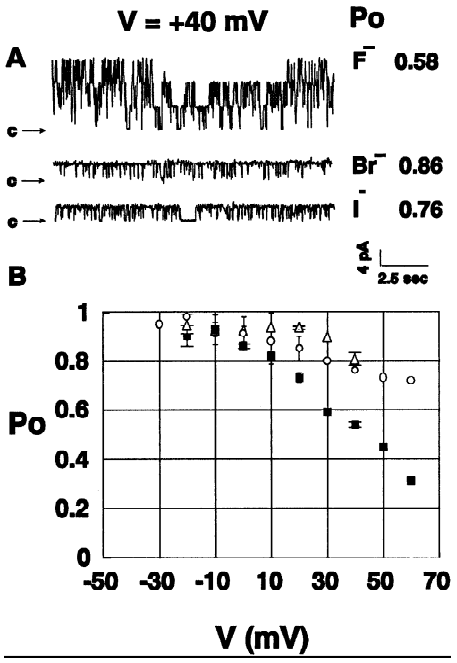

Fig. 6. Variation of P_o as a function of voltage. (*A*) Single-channel currents recorded in 200 mM KCl *cis*/50 mM KCl + 150 mM KX *trans* at +40 mV (X = Br, I, F). (*B*) P_o as a function of voltage: 200 mM KCl *cis*/50 mM KCl + 150 mM KX *trans* (X = Br (▽), I (○), F (■)).

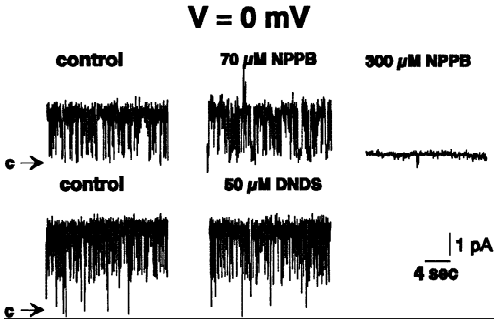

Fig. 7. The blocking effect of NPPB and DNDS on Cl^--selective channels. Single-channel recordings under control conditions, and immediately after *cis* addition of 70 μM and 300 μM NPPB. There was no apparent inhibition of channel activity in the presence of 50 μM DNDS in the *trans* chamber. Single-channel currents were recorded in asymmetrical conditions (200 mM KCl *cis*/50 mM KCl *trans*) at $V = 0$ mV.

Channel Block

The pharmacological properties of the voltage-sensitive Cl^- channel in RER vesicles were investigated by testing the blocking effect of specific agents such as NPPB and DNDS. Figure 7 shows that the addition of 70 μM NPPB to the *cis* chamber reduced the channel P_o from 0.9 to 0.75 at 0 mV. The blocking effect of NPPB was characterized by an increased fast flickering and longer silent periods. Total block was observed with 300 μM NPPB in the *cis* chamber. In contrast, DNDS failed to cause channel inhibition when applied at a *trans* concentration of 50 μM.

Several reports have indicated that divalent anions constitute potent blocking agents of Cl^- channels. *I/V* curves measured in 200 mM *cis*/50 mM *trans* KCl (filled circles) and in 200 mM *cis*/50 mM KCl *trans* + 25 mM NaH_2PO_4 *trans* (open circles) conditions are presented in Fig. 8. At pH 7.4, phosphate is present as HPO_4^{2-} + $H_2PO_4^-$ in a 3:2 ratio. The curves in Fig. 8 show that addition of phosphate decreased the current amplitude at potentials more negative than 40 mV, without apparent effects on the zero current potential value. Figure 9*A* and *B* illustrates the effect of 50 mM *trans* NaH_2PO_4 on channel fluctuations and the dose-dependent blocking action of phosphate on Cl^- channels at 0 mV. These observations led to the conclusion that part of the action of phosphate consisted of a reversible reduction of the

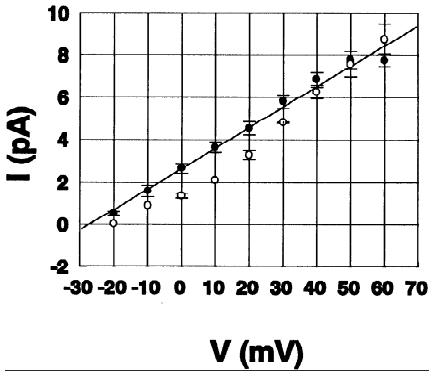

Fig. 8. Single-channel current-voltage relationship in 200 mM KCl *cis*/50 mM KCl *trans* (●) and in 200 mM KCl *cis*/50 mM KCl + 25 mM NaH_2PO_4 *trans* (○) conditions. The presence of NaH_2PO_4 did not have any apparent effect on the zero current potential value. Data points are mean ± SE of 4 different experiments.

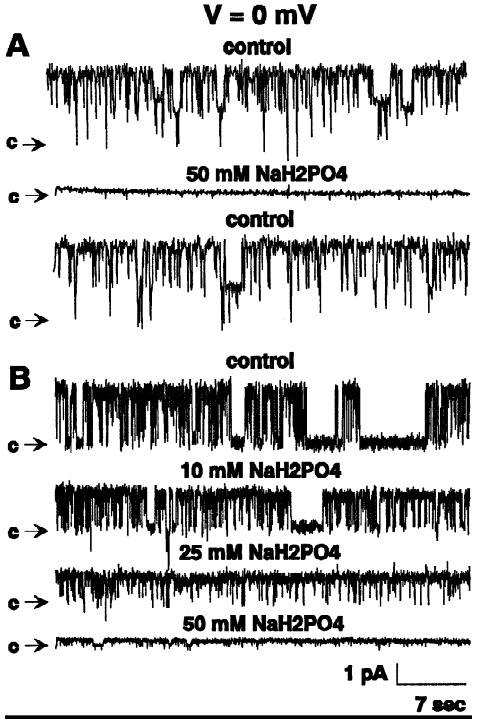

Fig. 9. Effect of NaH_2PO_4 on a Cl^- channel at 0 mV. (*A*) Channel recording under control conditions (200 mM KCl *cis*/50 mM KCl *trans*), immediately after addition of 50 mM NaH_2PO_4 to the *trans* chamber and after perfusion of the chamber with a phosphate-free control solution. (*B*) Single-channel currents recorded in control conditions (200 mM KCl *cis*/50 mM KCl *trans*) and after addition of various concentrations of NaH_2PO_4 in *trans*. NaH_2PO_4 decreased the current amplitude in a dose dependent manner.

channel unitary current amplitude, a result compatible with the expected effect of a fast blocking agent. Figure 10*A* illustrates the dose-response curve of the I/I_o ratio, where I_o and I represent the channel unitary current amplitude in the absence and in the presence of phosphate respectively, as a function of the *trans* phosphate concentration. These data indicate that the observed decrease in current amplitude is a function of the phosphate concentration with a half inhibition concentration at 0 mV of 25 mM. The voltage dependence of the I/I_o ratio measured at two different Cl^- concentrations is presented in Fig. 10*B*. With 25 mM NaH_2PO_4 and 50 mM Cl^- in *trans* (filled circles), the inhibitory action of phosphate appeared clearly voltage dependent with I/I_o values decreasing significantly at potentials more negative than 40 mV. An analysis based on the model proposed by Woodhull (1973), [33] showed that the data in Fig. 10*B* can be approximated by a Boltzmann equation of the form

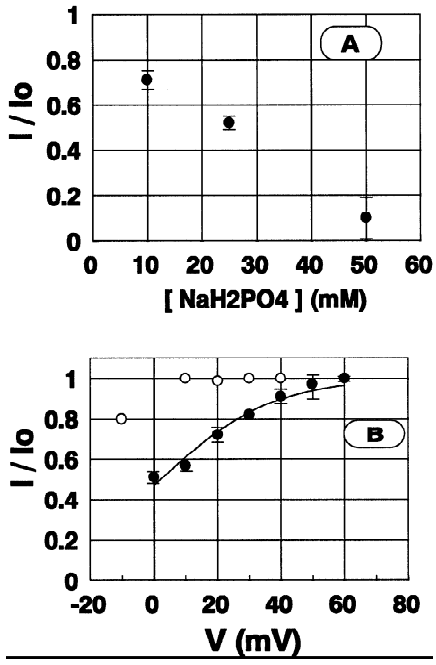

Fig. 10. Voltage dependent block of NaH_2PO_4. (*A*) Relationship between the current amplitude I/I_o ratio and the *trans* NaH_2PO_4 concentration with I_o and I representing the current amplitude in the absence and in the presence of NaH_2PO_4. Measurements were carried out on 4 different bilayers. All experiments were done under 200 mM KCl *cis*/50 mM KCl + various *trans* NaH_2PO_4 concentrations at 0 mV. Half inhibition was observed at 25 mM NaH_2PO_4. (*B*) I/I_o ratio as a function of voltage under 200 mM KCl *cis*/50 mM KCl + 25 mM NaH_2PO_4 *trans* (n = 4) (●) and 200 mM KCl symmetrical conditions +25 mM NaH_2PO_4 *trans* (n = 1) (○). The inhibitory effect of NaH_2PO_4 is voltage dependent and can be partially reversed in the presence of 200 mM KCl *trans.*

$$\frac{I}{I_o} = \frac{1}{\left(1 + e^{\frac{Zdq(V - V_o)}{KT}}\right)} \qquad (2)$$

with V_o = 2.3 mV and Zd = 1.43. A value for Zq > 1

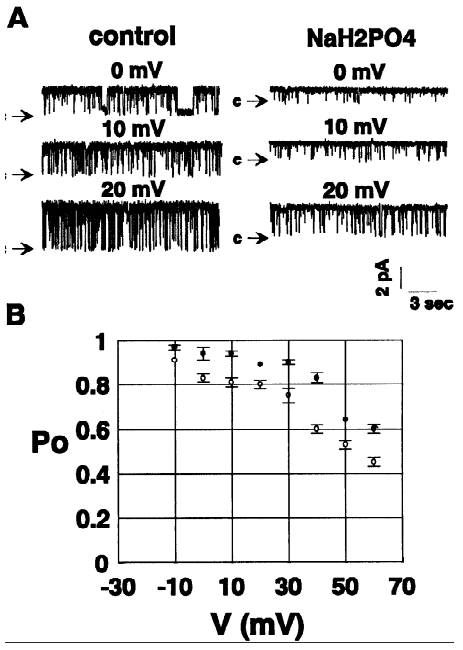

Fig. 11. The effect of NaH_2PO_4 on the channel P_o as a function of voltage. (*A*) The effect of NaH_2PO_4 on channel-gating behavior obtained under control conditions (200 mM KCl *cis*/50 mM KCl *trans*) and in the presence of NaH_2PO_4 (200 mM KCl *cis*/50 mM KCl + 25 mM Na H_2PO_4 *trans*). Long silent periods and faster flickering are decreased by NaH_2PO_4. (*B*) Open channel as a function of membrane voltage under above conditions (○: control, ●: in presence of NaH_2PO_4). There was an increase of the channel mean P_o value ($n = 3$) in the presence of NaH_2PO_4.

suggests that channel block involves the interaction of doubly charge phosphate (HPO_4^{2-}) with a site located at 70% of the membrane span. In contrast, the presence of 200 mM KCl with 25 mM NaH_2PO_4 (open circles) in the *trans* compartment resulted in a reduction of the blocking action of phosphate. Finally, the effect of phosphate on the channel open probability as a function of voltage is illustrated in Fig. 11*A* and *B*. The mean value of P_o ($n = 3$), slightly increased in the presence of phosphate (filled circles), indicating that, in addition to an effect on the channel unitary current amplitude, phosphate appears also to modify the channel gating process, with *trans* phosphate inducing an enhanced channel activity.

Discussion

The present work reports the basic characterization of an anion-selective channel obtained by fusion of RER vesicles from rat hepatocytes into POPE/POPC bilayers. The identified channel showed a selectivity sequence corresponding to $P_{Br} > P_{Cl} > P_I \approx P_F$, and a fluctuation pattern compatible with a kinetic scheme containing a single open state and a minimum of three closed states. The channel open probability appeared voltage dependent with higher P_o values at positive applied potentials. Evidence was also presented indicating a voltage dependent block by phosphate, suggesting the presence of a binding site located at an electrical distance equal to 70% of the membrane span from the *cis* side.

Channel Conductance and Voltage Dependence

The channel reported in this work has a single-channel conductance of 164 pS in symmetrical 200 mM KCl with P_o varying from 0.9 at 0 mV to 0.4 at +60 mV in 200 mM *cis*/50 mM *trans* KCl conditions. In one occasion we measured a channel of identical conductance but with an opposite voltage dependence. This single observation was interpreted as resulting from an inverse channel orientation upon fusion into the planar bilayer, and confirmed because of its low occurrence, the morphological measurements of Paiement and Bergeron (1983), [17] supporting a right-side out configuration for the RER vesicles used. A K^+ selective channel of small conductance (10 pS in 200 mM KCl) was also observed in 10 different bilayers. This channel appeared Ca^{2+} insensitive and could not be blocked by either TEA (10 mM) or Ba^{2+} (10 mM). The results in Fig. 2 show that the dwell time distribution of the open intervals for the Cl^- channel can be accounted for by a single exponential function while the distribution of the closed intervals required at least three different states. It is clear also from this figure that the occupancy of the long lasting closed state is increased at more positive potential values. Additional observations indicated also that the mean closed time increased at positive potentials while there was a decrease of the mean open time over the same voltage range (Fig. 4). These findings suggest that the voltage dependence of P_o in fact results from the appearance at positive potentials of long silence periods coupled to shorter open time and longer closed time intervals during channel bursts. Voltage-gated Cl^- channels have already been identified in several internal organelles. For instance, a 300 pS channel (150 mM KCl) slightly more selective for anions than cations was reported in RER membrane vesicles from canine pancreas [26]. This channel was open most of the time at negative potentials (*cis* relative to *trans*) and largely closed at positive potential values. Such a behavior cannot account for the results presented in Fig. 3*B*. Similarly, a 260 pS anion channel was measured in giant liposomes made of ER from rat exocrine pancreas [24]. This channel showed, in symmetrical salt solutions, a maximal open probability at 0 mV that declined for voltages with ± 20 mV. A 130 pS Cl^- channel (symmetrical 250 mM KCl) was also characterized by Townsend and Rosenberg (1995) [31]

in cardiac SR with a voltage dependency opposite to that presented in Fig. 3*B*. Schmid et al., (1989) [23] have reported in a study on endosomal vesicles from rat kidney cortex, the presence of a 73 pS Cl^- channel with a mean open time increasing at positive applied potentials. Such a behavior is at variance with the findings illustrated in Fig. 4*A* of the present work. Finally, a Cl^- selective channel of 150 pS activated at negative potentials (lumen relative to cytosol) was described by Tabaras et al. (1991) [27] in the nuclear membrane of liver cells. This channel presents conductance properties and a voltage dependence which are in accordance with the results presented in this work. Such an agreement is not unexpected considering that in most cells, the outer nuclear membrane is continuous with the RER. It should be noticed that because of the limited voltage range used in our experiments at negative potential values (Fig. 3*B*) our observations do not rule out a possible decrease of the channel P_o at these voltages. Furthermore, because the absolute *trans* Cl^- concentration has been found to affect the gating process of several Cl^--selective channels [19, 32], the fact that most of our experiments were performed in 200 mM KCl *cis*/50 mM KCl *trans* conditions and not in symmetrical KCl (200 mM) solutions, limits the comparisons that can be made between the P_o voltage dependence presented in this work and the results from the other preparations described here. The present observations remain nevertheless compatible with the results obtained in a related work on rat liver RER vesicles where each monomer of a double-barreled Cl^- channel showed a P_o *vs.* voltage relationship with characteristics similar to the ones presented in Fig. 3*B* [15]. A double-barreled type fluctuation pattern was not however observed in the present case. A binomial analysis of current records such as that illustrated in Fig. 3*A* (*data not shown*), indicated that our results support a system in which two identical 164 pS channels fluctuate independently. The absence of double-barreled behavior in the present case may be partially related to differences in experimental conditions such as charged (PG) vs neutral (PE/PC)) lipids and/or Cl^- ion concentrations. An effect of the Cl^- ion transmembrane gradient on *Torpedo* Cl^- channel double-barreled kinetics has already been reported [14]. Because previous measurements were carried out in 450 mM *cis*/50 mM *trans* KCl conditions, the possibility that the appearance of a double-barreled system was favored by a high Cl^- ion gradient can not be ruled out [15]. In addition, the presence of a negative surface potential resulting from use of a charged phospholipid such as PG provided conditions where the *trans* Cl^- concentration near the membrane interface was substantially smaller than that of the bulk (6 mM with 50 mM bulk and a surface potential of −53 mV: *see* [22]). Our results show that channel gating is affected by the permeant ion in *trans*, suggesting that under low Cl^- ion conditions the channel kinetic scheme may be modified.

Channel Selectivity

The channel obtained from RER was found to be highly selective for chloride over potassium ($P_{Cl}/P_K > 10$) with a permeability sequence for anions given by Br^- (1.3) > Cl^- (1) > I^- (0.45) = F^- (0.50). This channel appears more anion selective than the Cl^- channel measured by Schmid and coworkers (1989) [23] in endosomal vesicles from rat kidney cortex, and presents a permeability sequence different from that reported by Townsend and Rosenberg (1995), [31] in their study on cardiac sarcoplasmic reticulum where a permeability ratio $P_I/P_{Cl} > 1$ was observed. The 164 pS channel described in this work also differs from the outward rectifying Cl^- channels identified in a large variety of cellular preparations and which show a permeability sequence characteristic of the Eisenman III series ($P_{Br} > P_{Cl} > P_I > P_F$) [4, 13]. In addition, Fig. 6*A* and *B* provides evidence that the voltage dependence of P_o estimated from recordings where the long closed times were included, was affected by the presence of 150 mM *trans* halide ions. For instance, the P_o values measured with Br^- ions was clearly higher than with F^-. In this case, the selectivity of conductance was reflected in the ion selectivity of gating. One may therefore hypothesize that this channel contains anion-selective sites which can modulate channel gating. Accordingly, less permeant ions such as F^- are not expected to affect the channel gating process because of their limited access to the sites. Our results are thus in agreement with the findings reported for halide anions on the gating properties of the *Torpedo* electric organ Cl^--channel ClC-0 [19]. This proposal also suggests that increasing the Cl^- concentration in *trans* should promote channel opening. Experiments carried out in symmetrical 200 mM KCl (*data not shown*) provided preliminary evidence that the P_o values measured under these conditions approximate the values obtained with Br^- in *trans* solution as illustrated in Fig. 6*B*. Less conclusive results were obtained, however, using I^-. The P_o values observed in the presence of *trans* I^- were not significantly different from that estimated in Br^- conditions, despite evidence for a permeability ratio $P_{Br}/P_I > 1$ (Fig. 5*B*). These results suggest that I^- interferes in multiple ways with both channel gating and channel conductance. The possibility that, as for CFTR Cl^- channels, I^- acts through a blocking action cannot be currently ruled out [28].

Channel Block

The channel pharmacological properties were investigated by testing the effect of NPPB and DNDS. The application of 70 μM NPPB was found to decrease channel open probability from 0.9 to 0.75 at 0 mV by induc-

ing fast flickering. We also observed that channel activity was totally blocked using 300 μM NPPB. This result is similar to that reported by Schmid et al. [23], in their study on endosomal vesicles from rat kidney cortex where total inhibition was measured at 100 μM NPPB. A greater NPPB sensitivity was reported by Townsend and Rosenberg [31] in their study on cardiac SR with half inhibition obtained at 52.6 μM NPPB. In contrast the 260 pS channel identified by Schmid et al. [24] on giant liposomes from rat exocrine pancreas ER could not be inhibited by NPPB at concentrations of 100 μM. In the present case, we could not detect a blocking action of DNDS when applied at a *trans* concentration of 50 μM. A fast blocking action of DNDS characterized by a decrease of the channel unitary amplitude was observed on Cl^- channels from SR membrane preparations [10, 31] at concentrations > 100 μM, but studies on outward rectifying Cl^--selective channels showed inhibition of channel activity at DNDS concentrations as low as 3.7 μM. These data indicate that the Cl^- channel identified in this work display a low sensitivity to this agent [20].

Blocking Effect of Phosphate

We found that *trans* phosphate inhibited Cl^- currents reversibly (Figs. 9 and 10). It was concluded on the basis of Fig. 10*B* that phosphate blocks the channel according to a competitive blocking model with a binding site located at an equivalent electrical distance $Zd = 1.4$ and with a dissociation constant for phosphate equal to 25 mM. According to that model, phosphate would enter the channel from the *trans* side, bind to a Cl^- binding site and consequently block the flow of Cl^- through the channel. Increasing the *trans* Cl^- concentration under these conditions would prevent phosphate binding resulting in an impaired blocking action of phosphate as illustrated in Fig. 10*B*. In addition, an equivalent charge greater than 1 (1.4 q) rules out a potential contribution of $H_2PO_4^-$ as the blocking agent, but strongly suggests a blocking action coming from the divalent anion HPO_4^{2-} at a site located at distance corresponding to 70% of the membrane span from the *cis* side. The possibility that $H_2PO_4^-$ could permeate the channel cannot be ruled out, since the experimental conditions used to estimate the shift in reversal potential in the presence of trans phosphate (Fig. 8) are limited to low phosphate concentrations due to the important channel block at phosphate concentrations > 50 mM. The effects of phosphate appear not to be limited to a decrease of the channel current jump amplitude. Figure 11 reveals that *trans* application of phosphate resulted in a significant increase of the channel P_o as a function of voltage. Similar findings were presented in Fig. 6*B*, where the permeant anion Br^- but not F^- was found to increase P_o at positive potentials. This phenomenon cannot be related to a change of the *trans* solution ionic strength, since the results in Fig. 6*B* obtained in the presence of F^- failed to indicate a positive shift of the P_o *vs.* voltage relationship under similar ionic strength conditions. These two effects, namely the fast blockade by phosphate observed at −40 up to 20 mV (Fig. 9*A* and *B;* Fig. 10*B*) and the phosphate-dependent variations of P_o measured at all experimental potentials may be interpreted in terms of a model in which the luminal segment (*trans* side) of the channel contains two binding sites for phosphate; one binding site located in the ion conducting pathway that would be involved in blocking process by HPO_4^{2-} and a second binding site that would be responsible for the effect of $H_2PO_4^-$ on the channel gating process as observed with the permeant anion Br^-.

Conclusions

We have characterized a Cl^- channel from liver cell RER. This channel is Cl^- selective and affected by membrane voltage and phosphate ions. Increasing evidence suggests that the ER has an important role in the regulation of cytosolic free Ca^{2+} concentrations in a variety of non-muscle cells. The release of Ca^{2+} from the ER would likely lead to a luminal potential negative with respect to the cytoplasm, thus limiting Ca^{2+} efflux. Our results showed that the Cl^- channel remained very active within the voltage range ± 20 mV. It has been suggested that Cl^- ion movement through ER Cl^- channels attenuates the negative potential related to Ca^{2+} release by acting as a counterion. The importance of this mechanism remains to be established, the actual concentration of Cl^- in the ER being unknown. Previously, Fulceri and coworkers [8] demonstrated that glucose-6-phosphatase stimulates the MgATP-dependent Ca^{2+} uptake by liver microsomes. Their results suggested that such a stimulatory effect was due to the supply of phosphate ions inside the microsomal vesicles, through the glucose 6-phosphatase mediated hydrolysis of glucose 6-phosphate, and that the phosphate ions so supplied act as physiological entrapping agents by interacting with the actively transported Ca^{2+}. Our results do not rule out that the Cl^- channel identified in this work may constitute a permeation pathway for $H_2PO_4^-$. However, the passage of $H_2PO_4^-$ and Cl^- through this channel will be a function of the lumen concentration of HPO_4^{2-} in the RER.

This work was supported by a grant from the Medical Research Council of Canada. The authors also acknowledge the technical assistance of Dr. J. Paiement for the preparation of the vesicles.

References

1. Anderson, M.P., Sheppard, D.N., Berger, H.A., Welsh, M.J. 1992. Chloride channels in the apical membrane of normal and cystic

fibrosis airway and intestinal epithelia. *Am. J. Physiol.* **263:**L1–L14

2. Bayerdorffer, E., Streb, H., Eckhardt, L., Hasse, W., Schulz, I. 1984. Characterization of calcium uptake into rough endoplasmic reticulum of rat pancreas. *J. Membrane Biol.* **81:**69–82
3. Bellemare, F., Morier, N., Sauvé, R. 1992. Incorporation into a planar lipid bilayer of K channels from the luminal membrane of rabbit proximal tubule. *Biochim. Biophys. Acta* **1105:**10–18
4. Cahalan, M.D., Lewis, R.S. 1988. Role of potassium and chloride channels in volume regulation by T lymphocytes. *In: Cell Physiology of Blood.* R. Gunn and J. Parker, editors. pp. 281–301. Rockefeller Univ. Press, New York
5. Colombini, M. 1983. Purification of VDAC (Voltage-Dependent Anion-Selective Channel) from rat liver mitochondria. *J. Membrane Biol.* **74:**115–121
6. Denicourt, N., Cai, S., Garneau, L., Gagnan-Bruentte, M., Sauvé, R. 1996. Evidence from incorporation experiments for an anionic channel of small conductance at the apical membrane of the rabbit distal tubule. *Biochim. Biophys. Acta* **1285:**155–166
7. Franciolini, F., Petris, A. 1990. Chloride channels of biological membranes. *Biochim. Biophys. Acta* **1031:**247–259
8. Fulceri, R., Bellomo, G., Gamberucci, A., Benedetti, A. 1990. MgATP-dependent accumulation of calcium ions and inorganic phosphate in a liver reticular pool. *Biochem. J.* **272:**549–552
9. Glickman, J., Croen, K., Kelly, S., Al-Awqati, Q. 1983. Golgi membranes contain an electrogenic H^+ pump in parallel to a chloride conductance. *J. Cell Biol.* **97:**1303–1308
10. Hals, G.D., Stein, P.G., Palade, P. 1989. Single-channel characteristics of a high conductance anion channel in ~sarcoballs~. *J. Gen. Physiol.* **93:**385–410
11. Kan, F.W.K., Jolicoeur, M., Paiement, J. 1992. Freeze-fracture analysis of the effects of intermediates of the phosphatidylinositol cycle on fusion of rough endoplasmic reticulum membranes. *Biochim. Biophys. Acta* **1107:**331–341
12. Macknight, A. 1988. Principles of cell volume regulation. *Renal Physiol. Biochem.* **11:**114–141.
13. McDonald, T.V., Nghiem, P.T., Gadner, P., Martens, C.L. 1992. Human lymphocites transcribe the cystic fibrosis transmembrane conductance regulator gene and exhibit CF-defective cAMP-regulated chloride current. *J. Biol. Chem.* **267:**3242–3248
14. Miller, C., Richard, E.A. 1990. The voltage-dependent chloride channel of the Torpedo electroplax: intimations of molecular structure from quirks of single-channel function. *In: Cloride Channels and Carriers in Nerve, Muscle and Glial Cells.* F.J. Alvarez-Leefmans and J.M. Russell, editors. pp. 383–405. Plenum Press, New York
15. Morier, N., Sauvé, R. 1994. Analysis of a novel double-barreled anion channel from rat liver rough endoplasmic reticulum. *Biophys. J.* **67:**590–602
16. Nelson, D.J., Tang, J.M., Palmer, L.G. 1984. Single-channel recording of apical membrane chloride conductance in A6 epithelial cells. *J. Membrane Biol.* **80:**81–89
17. Paiement, J., Bergeron, J.J. 1983. Localization of GTP-stimulated core glycolysation to fused microsomes. *J. Cell Biol.* **96:**1791–1796
18. Palade, P., Dettbarn, C., Volpe, P., Alderson, B., Otero, A.S. 1989. Direct inhibition of inositol-1,4,5-trisphosphate-induced Ca^{2+} release from brain microsomes by K^+ channel blockers. *American Soc. for Pharm. & Exp. Therapeutics* **36:**664–672
19. Pusch, M., Ludewig, U., Rehfeldt, A., Jentsch, T.J. 1995. Gating of the voltage-dependent chloride channel ClC-0 by the permeant anion. *Nature* **373:**527–531
20. Reinhardt, R., Bridges, R.J., Rummel, W., Lindemann, B. 1987. Properties of an anion-selective channel from rat colonic enterocyte plasma membranes reconstituted into planar phospholipid bilayers. *J. Membrane Biol.* **95:**47–54
21. Rousseau, E. 1989. Single chloride-selective channel from cardiac sarcoplasmic reticulum studied in planar lipid bilayers. *J. Membrane Biol.* **110:**39–47
22. Sauvé, R., Ohki, S. 1979. Interactions of divalent cations with negatively charged membrane surfaces. I. Discret charge potential. *J. Theor. Biol.* **81:**157–179
23. Schmid, A., Burckhardt, G., Gogelein, H. 1989. Single chloride channels in endosomal vesicle preparations from rat kidney cortex. *J. Membrane Biol.* **111:**265–275
24. Schmid, A., Gogelein, H., Kemmer, T.P., Schulz, I. 1988. Anion channels in giant liposomes made of endoplasmic reticulum vesicles from rat exocrine pancreas. *J. Membrane Biol.* **104:**275–282
25. Shah, J., Pant, H.C. 1988. Potassium-channel blockers inhibit inositol trisphosphate-induced calcium release in the microsomal fractions isolated from the rat brain. *Biochem. J.* **250:**617–620
26. Simon, S.M., Blobel, G., Zimmerberg, J. 1989. Large aqueous channels in membrane vesicles derived from the rough endoplasmic reticulum of canine pancreas or the plasma membrane of Escherichia coli. *Proc. Natl. Acad. Sci. USA* **86:**6176–6180
27. Tabares, L., Mazzanti, M., Clapham, D.E. 1991. Chloride channels in the nuclear membranes. *J. Membrane Biol.* **123:**49–54
28. Tabcharani, J.A., Chang, X.-B., Riordan, J.R., Hanrahan, J.W. 1992. The cystic fibrosis transmembrane conductance regulator chloride channel. Iodide block and permeation. *Biophys. J.* **62:**1–4.
29. Tanifuji, M., Sokabe, M., Kasai, M. 1987. An anion channel of sarcoplasmic reticulum incorporated into planar lipid bilayers:Single-channel behavior and conductance properties. *J. Membrane Biol.* **99:**103–111
30. Tilly, B.C., Mancini, G.M., Bijman, J., van Gageldonk, P.G., Beerens, C.E., Bridges, R.J., De Jonge, H.R., Verheijen, F.W. 1992. Nucleotide-activated chloride channels in lysosomal membranes. *Biochem. Biophys. Res. Comm.* **187:**254–260
31. Townsend, C., Rosenberg, R.L. 1995. Characterization of a chloride channel reconstituted from cardiac sarcoplasmic reticulum. *J. Membrane Biol.* **147:**121–136
32. Winters, C.J., Reeves, W.B., Andreoli, T.E. 1990. Cl^- channels in basolateral renal medullary membrane: III. Determinants of single-channel activity. *J. Membrane Biol.* **118:**269–278
33. Woodhull, A.M. 1973. Ionic blockage of sodium channels in nerve. *J. Gen. Physiol.* **61:**687–708